Monounsaturated PE Does Not Phase-Separate from the Lipid Raft Molecules Sphingomyelin and Cholesterol: Role for Polyunsaturation?†

Saame Raza Shaikh,[‡,§] Michael R. Brzustowicz,[§,||] Noah Gustafson,[||] William Stillwell,[‡,§] and Stephen R. Wassall*[,§,||]

Department of Biology, Indiana University Purdue University Indianapolis, 723 West Michigan Street, Indianapolis, Indiana 46202-5132, Department of Physics, Indiana University Purdue University Indianapolis, 402 North Blackford Street, Indianapolis, Indiana 46202-3273, and Medical Biophysics Program, Indiana University School of Medicine, 635 Barnhill Drive, Indianapolis, Indiana 46202-5122

Received February 20, 2002; Revised Manuscript Received June 5, 2002

ABSTRACT: We investigated interactions of the lipid raft molecules sphingomyelin (SM) and cholesterol (CHOL) in monolayers and bilayers composed of 1-palmitoyl-2-oleoyl-*sn*-glycerophosphatidylethanolamine (POPE) or 1-palmitoyl-2-docosahexaenoyl-*sn*-glycerophosphatidylethanolamine (PDPE) at 35 °C. Techniques employed were pressure−area ($\pi-A$) isotherms generated from Langmuir−Blodgett films, solid-state ^{2}H and ^{31}P NMR spectroscopies, and differential scanning calorimetry (DSC). Condensation calculated from $\pi-A$ isotherms and reduction in the enthalpy of the gel−liquid-crystalline transition in DSC scans showed CHOL has a strong affinity for POPE, comparable to that observed between SM−CHOL. Order parameters derived from ^{2}H NMR spectra of the perdeuterated *sn*-1 chain of POPE-d_{31} increased by >50% upon addition of equimolar CHOL to POPE-d_{31}/SM (1:1 mol) bilayers. Close proximity of CHOL to POPE even in the presence of SM is indicated. Chemical shift anisotropy ($\Delta\sigma_{csa}$) measured from ^{1}H-decoupled ^{31}P NMR spectra also implied intimate lipid mixing in POPE/SM/CHOL (1:1:1 mol). In contrast, $\pi-A$ isotherms and corroborating DSC studies of PDPE/SM (1:1 mol) indicate phase separation between SM and PDPE, which was maintained in the presence of CHOL. The cholesterol-associated increase in order of the perdeuterated *sn*-1 chain of PDPE determined by ^{2}H NMR was 2-fold less for PDPE-d_{31}/SM/CHOL (1:1:1 mol) than POPE-d_{31}/SM/CHOL (1:1:1 mol). Our findings support the notion that acyl chain dependent lateral phase separation occurs in the presence of a docosahexaenoic acid (DHA)-containing phospholipid (PDPE), but not an oleic acid-containing phospholipid (POPE). We propose that monounsaturated lipids do not promote formation of stable lipid rafts and that polyunsaturation may be important for raft stability.

The lipid component of the mammalian plasma membrane contains hundreds of different types of lipid species that work together to provide a fluid hydrophobic environment for protein functionality. The array of lipids found in the plasma membrane can be generally categorized into three types: phospholipids, sphingolipids, and cholesterol. Sphingolipids comprise 10−20 mol % of the plasma membrane (*1*) and the cholesterol content can be as high as 50 mol % (*2*), while the remaining lipids are predominantly phospholipids. It has become universally accepted that the lipids in the plasma membrane are not distributed homogeneously (*3*−*6*). Evidence from both in vitro (*4*) and in vivo (*7*) studies show that lipids, as well as proteins, are organized into distinct patches referred to as membrane microdomains. Formation of stable laterally phase-separated lipid microdomains is promoted by the differential affinities between specific lipid molecules. Historically, much of the evidence for lipid microdomains has come from phase separations in model membranes between lamellar gel (L_β)[1] and lamellar liquid-crystalline (L_α) state lipids (*6*). Although such studies have provided much insight, their biological relevance has remained limited since few gel-state lipids are found in biological membranes.

Recently, a great deal of focus has been upon specialized mammalian plasma membrane lipid microdomains that are rich in sphingolipids and cholesterol and are referred to as lipid rafts (*8*, *9*). Lipid rafts exist in a liquid-ordered (l_o) state (*8*), an intermediate state between the conventionally named L_β and L_α states that have also been designated solid-ordered (s_o) and liquid-disordered (l_d), respectively. The l_o state is characterized by high acyl chain order similar to the L_β phase but with rapid axial rotation and high lateral mobility as in the L_α state (*8*, *10*). Much of the evidence for lipid rafts has come from low-temperature (4 °C) detergent isolations (*11*)

† This work was supported by a grant from the National Institutes of Health (RO1CA57212).

* Corresponding author. Email: swassall@iupui.edu. Tel: 317 274-6908. Fax: 317 274-2393.

‡ Department of Biology, Indiana University Purdue University Indianapolis.

§ Medical Biophysics Program, Indiana University School of Medicine.

|| Department of Physics, Indiana University Purdue University Indianapolis.

[1] Abbreviations: CHOL, cholesterol; DSC, differential scanning calorimetry; L_α, lamellar liquid-crystalline phase; L_β, lamellar gel phase; l_d, liquid-disordered phase; l_o, liquid-ordered phase; MLV, multilamellar vesicle; PC, phosphatidylcholine; PDPE, 1-palmitoyl-2-docosahexaenoyl-*sn*-glycerophosphatidylethanolamine; PE, phosphatidylethanolamine; POPE, 1-palmitoyl-2-oleoyl-*sn*-glycerophosphatidylethanolamine; $\pi-A$, pressure−area; SM, sphingomyelin; T_m, gel to liquid-crystalline transition temperature.

10.1021/bi025712b CCC: $22.00 © 2002 American Chemical Society
Published on Web 07/27/2002

that produce patches of the cell membrane that are detergent-resistant (DRMs, detergent-resistant membranes) and enriched not only in sphingolipids and cholesterol but also in lipidated proteins as well (*12*). Specifically, DRMs accumulate glycosylphosphatidylinositol (GPI)-anchored proteins and doubly acylated kinases of the SRC family (*13*). Therefore, it is postulated that lipid rafts may serve as platforms for intracellular cell signaling by promoting protein−protein interactions (*9*).

Recent evidence utilizing new imaging techniques revealed that lipid rafts, ranging in size from 70 to 370 nm, exist in vivo for minutes as stable entities (*7*). Two general models have emerged to explain the relative stability of lipid rafts (*14*). The first model considers lipid headgroup interactions as the primary determinant of raft stability. By this model, stability is conferred by favorable interaction between the amide of the sphingosine backbone with the hydroxyl of an adjacent sphingolipid (*9*). Contributing to the stability of lipids rafts would be hydrogen bonding between the 3-OH of cholesterol with the sphingosine amide (*10*, *15*). The second model asserts that the primary feature of lipid raft formation appears to lie in acyl chain packing (*8*). It is postulated that saturated acyl chains promote formation of l_o rafts because the saturated acyl chains are more extended than the unsaturated chains and pack well among themselves as well as with cholesterol (*8*). Therefore, phospholipids with unsaturated acyl chains would be expected to phase-separate from the l_o domains and perhaps be a part of the detergent-soluble fraction (DSMs, detergent-soluble membranes). Here we test this hypothesis by assessing the interactions of the lipid raft components sphingomyelin (SM) and cholesterol (CHOL) on 1-palmitoyl-2-oleoyl-*sn*-glycerophosphatidylethanolamine (POPE) and 1-palmitoyl-2-docosahexaenoyl-*sn*-glycerophosphatidylethanolamine (PDPE) monolayers and bilayers.

PEs are the second most abundant type of phospholipids in the plasma membrane and are found predominantly as *sn*-1 saturated *sn*-2 unsaturated species. PEs have been shown to avoid cholesterol (*16*) whereas sphingolipids demonstrate high affinity for cholesterol (*17*). Therefore, it is reasonable to hypothesize that POPE and PDPE phospholipids would phase-separate from SM−CHOL-rich microdomains based on differential headgroup and acyl chain affinities. We employed solid-state ^{2}H and ^{31}P NMR spectroscopies, differential scanning calorimetry (DSC), and Langmuir−Blodgett films to follow the interactions between POPE or PDPE and the lipid raft molecules SM and CHOL. Our findings, however, show that that the oleic acid-containing phospholipid POPE does not phase-separate from SM−CHOL microdomains whereas the docosahexaenoic acid (DHA)-containing phospholipid PDPE may. This evidence supports the model that acyl chain packing is the key determinant in promoting lateral phase separations into stable SM−CHOL-rich and SM−CHOL-poor microdomains.

EXPERIMENTAL PROCEDURES

Materials. Egg sphingomyelin (SM), 1-palmitoyl-2-oleoyl-*sn*-glycero-phosphatidylethanolamine (POPE), 1-[$^2H_{31}$]palmitoyl-2-oleoyl-*sn*-glycerophosphatidylethanolamine (POPE-d_{31}), 1-palmitoyl-2-docosahexaenoyl-*sn*-glycerophosphatidylethanolamine (PDPE), and 1-[$^2H_{31}$]palmitoyl-2-docosahexaenoyl-*sn*-glycerophosphatidylethanolamine (PDPE-d_{31}) were purchased from Avanti Polar Lipids (Alabaster, AL). Cholesterol (CHOL) was obtained from Sigma Chemical Co. (St. Louis, MO). [3α-$^2H_1$]Cholesterol deuterated at the 3α position was synthesized from 5-cholestane-3-one (Steraloids, Newport, RI) and lithium aluminum deuteride (Sigma Chemical Co., St. Louis, MO) according to Oldfield et al. (*18*). Lipid purity was assessed with thin-layer chromatography. Lipid and cholesterol concentrations were quantified using phosphate and gravimetric analyses, respectively. All solvents were HPLC-grade and were purchased from Aldrich Chemical (Milwaukee, WI). Water utilized for buffer solutions for $\pi-A$ isotherms, DSC, and ^{31}P NMR experiments was deionized, glass-distilled and run through a Milli-Q Plus Water Purification System (Millipore, Milford, MA). Deuterium-depleted H_2O (DDW) (Isotec Inc., Miamisburg, OH) was utilized in place of H_2O for ^{2}H NMR samples.

Lipid Monolayer Studies. Pressure−area ($\pi-A$) isotherms were obtained using a Mini Langmuir−Blodgett Trough (KSV Instruments, Helsinki, Finland) and a Wilhelmy plate. All equipment was rinsed with ethanol twice and 5 times with distilled water before use. Lipid monolayers composed of the appropriate mixture were spread on a 10 mM sodium phosphate buffer (pH 7.4) using hexane/2-propanol (3:2). The carrying solvent was allowed to evaporate for 5 min, and compression rates were set at ≤3 mN/m per minute. $\pi-A$ isotherms were acquired at 35 ± 0.5 °C using a temperature-regulated circulating water bath.

Analysis of $\pi-A$ Isotherms. Lipid area/molecule was calculated by linear extrapolation from the target pressure of 35 mN/m. The ideal mean molecular area $(A)_\pi$ of two-component mixed monolayers was calculated at a constant surface pressure (π) by

$$A_\pi = \chi_1(A_1)_\pi + (1 - \chi_1)(A_2)_\pi \quad (1)$$

where χ_1 is the mole fraction of component 1 and A_1 and A_2 are the mean molecular areas of pure components 1 and 2 at identical surface pressures (*19*). The area/lipid (phospholipid or sphingolipid), A_{lipid}, was calculated using

$$A_{lipid} = A_{obs} - A_{CHOL}\chi_{CHOL} \quad (2)$$

where A_{obs} is the experimentally observed area/molecule, A_{CHOL} is the mean molecular area of cholesterol, and χ_{CHOL} is the mole fraction of cholesterol. Percent condensation was calculated at a constant surface pressure using the equation:

$$\%\ \text{condensation} = \left[\frac{A_{ideal} - A_{obs}}{A_{ideal}}\right] \times 100 \quad (3)$$

where A_{ideal} is the ideal mean molecular area and A_{obs} is the experimentally obtained mean molecular area (*20*).

The $\pi-A$ data allowed for estimation of lipids lost (percent squeeze out) in the flat portions of the $\pi-A$ isotherms:

$$\%\ \text{squeeze out} = \left(1 - \frac{A_e}{A_b}\right) \times 100 \quad (4)$$

where A_b and A_e are the beginning and end, respectively, of the surface area of the near-horizontal (plateau) regions (*21*). The values for A_b and A_e were determined by drawing tangents on each side of the plateau region. Intersection of

the extrapolated tangents with an extrapolation of the near-horizontal region defined the plateau region.

Differential Scanning Calorimetry Studies. Lipids dissolved in chloroform were dried under nitrogen for 30 min followed by 12 h under vacuum to remove traces of organic solvents. Multilamellar vesicles (MLVs) were made by hydrating overnight the appropriate phospholipids at 10 mg/mL in 10 mM sodium phosphate, pH 7.4, and then oxygen was removed by purging the solution with nitrogen. MLVs were frozen in dry ice and thawed 3 times in a water bath above the gel−liquid-crystalline phase transition temperature (T_m) of the lipids. The MLV solutions (500 μL) were added to each of the three chambers of a Hart Scientific differential scanning calorimeter (Provo, UT) while the fourth chamber contained 500 μL of the buffer. Heating and cooling scans were made at 10 °C/h.

NMR Sample Preparation. Lipid mixtures were co-dissolved in chloroform, and the solvent was evaporated under a gentle stream of nitrogen. Because polyunsaturated phospholipids are prone to oxidation, all DHA sample preparation was done in a glovebox under a nitrogen atmosphere. The samples were placed under vacuum for 12 h to ensure the removal of trace organic solvent. The lipid mixtures were then hydrated to 50 wt % with 50 mM Tris buffer (pH 7.4) and vigorously vortexed for ~5 min. After pH correction, the samples were frozen and lyophilized at ~50 mTorr. For ^{2}H NMR samples, the lyophilization process was repeated 3 times in the presence of excess (2 mL) DDW to remove naturally abundant ^{2}HHO. After hydrating the powders to 50 wt %, the resultant aqueous multilamellar dispersions were transferred to 5 mm glass NMR tubes which were then fitted with a Teflon-coated plug. All samples were stored at −20 °C when not in use and were allowed to equilibrate to room temperature for ~1 h before experimentation.

The lipids within samples prepared in this manner are considered to be homogeneously mixed prior to hydration. In earlier work (*22*), we have compared phospholipid/cholesterol samples prepared as described here and by a low-temperature trapping (LTT) method (*23*) designed to ensure lipids do not demix during solvent removal. Essentially identical results were obtained.

NMR Spectroscopy. Solid-state ^{2}H NMR and ^{1}H-decoupled ^{31}P NMR spectra were acquired on a home-built spectrometer operating at resonance frequencies of 27.6 MHz (^{2}H) and 72.9 MHz (^{31}P with ^{1}H decoupling at 180 MHz) (*24*). A double resonance probe and a home-built probe (Cryomagnet Systems, Inc., Indianapolis, IN) with 5 mm transverse mounted coils and temperature control were utilized. Temperature was controlled at 35 ± 0.5 °C with a Love Controls (1600 series) temperature controller (Michigan City, IN). Experimental details and parameters for ^{2}H NMR (*22*, *24*) and ^{31}P NMR (*25*) experiments are as previously described.

Analysis of ^{2}H NMR Spectra. Order parameters, S_{CD}, for C−^{2}H bonds in [3α-^{2}H$_1$]CHOL, POPE-d_{31}, and PDPE-d_{31} were measured from the ^{2}H NMR spectra. The definition is

$$S_{CD} = \frac{1}{2}\langle 3\cos^2\beta - 1\rangle \tag{5}$$

where β is the time-dependent angle between the C−^{2}H bond and the bilayer normal, and the angular brackets denote a time average (*26*). Details of how S_{CD} was extracted from spectra and interpretation follow.

The order parameter S_{CD} of the 3α C−^{2}H bond for [3α-^{2}H$_1$]CHOL incorporated into bilayers was determined from the residual quadrupolar splitting

$$\Delta\upsilon_r = \frac{3}{4}\left(\frac{e^2qQ}{h}\right)|S_{CD}| \tag{6}$$

of the powder pattern spectrum recorded. An estimate of the most probable (tilt) angle α_0 of the sterol was derived from S_{CD} on the basis of a previously described model (*18*, *22*). In the model, the rigid steroid moiety rotates rapidly about its long molecular axis, and a Gaussian distribution of angles α is applied to the wobbling motion undergone by this axis relative to the bilayer normal.

Moments M_n were calculated from ^{2}H NMR spectra for POPE-d_{31} or PDPE-d_{31} with

$$M_n = \frac{\int_{-\infty}^{\infty}|\omega^n|f(\omega)\,d\omega}{\int_{-\infty}^{\infty}f(\omega)\,d\omega} \tag{7}$$

where ω is the frequency with respect to the central Larmor frequency ω_0, $f(\omega)$ is the line shape, and n is the order of the spectral moment (*26*). In practice, the integral is a summation over the digitized data. The expression

$$M_1 = \frac{\pi}{\sqrt{3}}\left(\frac{e^2qQ}{h}\right)|\bar{S}_{CD}| \tag{8}$$

relates the first moment M_1 to the average order parameter $\bar{S}_{CD}$ of the perdeuterated palmitic *sn*-1 chain via the static quadrupolar coupling constant (e^2qQ/h) = 167 kHz in the L_α phase. From $\bar{S}_{CD}$, the average acyl chain length, $\langle L\rangle$, was calculated by

$$\langle L\rangle = l(0.5 + |\bar{S}_{CD}|) \tag{9}$$

In this equation, l = 19.1 Å is the length of the chain projected onto the bilayer normal in the all-trans configuration (*27*, *28*). The average area/molecule A was then evaluated from the total volume of the acyl chains in a POPE molecule V = 905 Å^3 or PDPE molecule V = 948 Å^3 according to

$$A = \frac{V}{\langle L\rangle} \tag{10}$$

The estimate for V is the sum of the individual volumes for the CH, CH_2, and CH_3 segments in the palmitic, oleic, and docosahexaenoic chains in the L_α phase (*29*). Equation 10 assumes that *sn*-1 and *sn*-2 chains have the same average chain length.

Spectra for POPE-d_{31} were also FFT-depaked to enhance resolution. This procedure numerically deconvolutes the powder pattern signal to a spectrum representative of a planar membrane of single alignment (*30*). The depaked spectra consist of doublets with quadrupolar splittings $\Delta\nu(\vartheta)$ that equate to order parameters by

$$\Delta\nu(\theta) = \frac{3}{2}\left(\frac{e^2qQ}{h}\right)|S_{CD}|P_2(\cos\theta) \tag{11}$$

where $\vartheta = 0°$ is the angle the membrane normal makes with the magnetic field and $P_2(\cos \vartheta)$ is the second-order Legendre polynomial. Smoothed profiles of order along the perdeuterated palmitoyl *sn*-1 chain were then constructed assuming monotonic variation toward the disordered center of the bilayer (*31*).

Analysis of ^{31}P NMR Spectra. Chemical shift anisotropy:

$$\Delta\sigma_{csa} = \sigma_{||} - \sigma_{\perp} \quad (12)$$

where $\sigma_{||}$ and $\sigma_{\perp}$ specify the respective chemical shift for a membrane oriented so that the bilayer normal is parallel and perpendicular to the magnetic field, was evaluated by spectral simulation (*32*). Such an approach was necessary to analyze the two-component powder patterns obtained with POPE−SM mixtures. The adjustable parameters were $\Delta\sigma_{csa}$, isotropic chemical shift σ_{iso}, line broadening (Lorentzian or Gaussian), and intensity for each component. A least-squares criterion was employed to establish the best fit. Uncertainty in chemical shift anisotropy values was assessed to be ±0.2 ppm.

RESULTS AND DISCUSSION

POPE and SM Are Both Condensed by CHOL. We first assessed the differences in relative affinities between POPE−CHOL versus SM−CHOL mixtures in monolayers at 35 mN/m of surface pressure. We chose a lateral pressure of 35 mN/m because it is postulated to be similar to that of biological membranes (*33*). Figure 1 presents $\pi-A$ isotherms generated from Langmuir−Blodgett films at 35 °C for POPE (A) or SM (B) with increasing concentrations of cholesterol χ_{CHOL}. At 35 mN/m of surface pressure, the areas/molecule for POPE, SM, and CHOL were found to be 65.2, 61.1, and 38.8 Å^2, respectively. Increasing the amount of CHOL lowers the area/molecule for both POPE and SM (Table 1). Cholesterol, due to its rigid planar ring structure, occupies nearly the same area/molecule at all surface pressures (Figure 1), consistent with previous reports (*20*, *34*). Therefore, condensation values calculated (eq 1) for POPE−CHOL or SM−CHOL mixtures reflect condensation conferred by POPE or SM. At all levels of CHOL examined ($0.05 \leq \chi_{CHOL} \geq 0.50$), we found that SM was highly condensed, which is consistent with previous reports of a high degree of affinity between SM and CHOL (*16*) (Table 1). Interestingly, POPE also condensed with cholesterol, although less than that measured for SM. The greatest difference in condensation between POPE versus SM was found at $\chi_{CHOL} = 0.5$, where SM condensed by 18.7% and POPE by 12.6%.

POPE and CHOL Are Miscible in Bilayers. The affinity of CHOL and POPE in bilayers was further evaluated by changes in POPE thermotropic phase behavior with increasing χ_{CHOL} using DSC. Figure 2 shows the effect of 0.0−0.10 mol fraction CHOL on DSC heating scans of MLVs made from POPE ($T_m = 25.5$ °C). As little as $\chi_{CHOL} = 0.0050$ lowers the POPE phase transition (decrease in enthalpy), and by $\chi_{CHOL} = 0.10$, the phase transition is nearly obliterated and the T_m is shifted to a lower temperature (22.6 °C). We previously reported a similar trend with SM−CHOL mixtures (*34*). SM exhibited a broad transition with a $T_m = 39.5$ °C (*34*). Addition of $\chi_{CHOL} = 0.01$ to SM lowered the SM phase transition, and by $\chi_{CHOL} = 0.10$, the SM phase transition was also shifted to a lower T_m (37.8 °C) and nearly obliterated

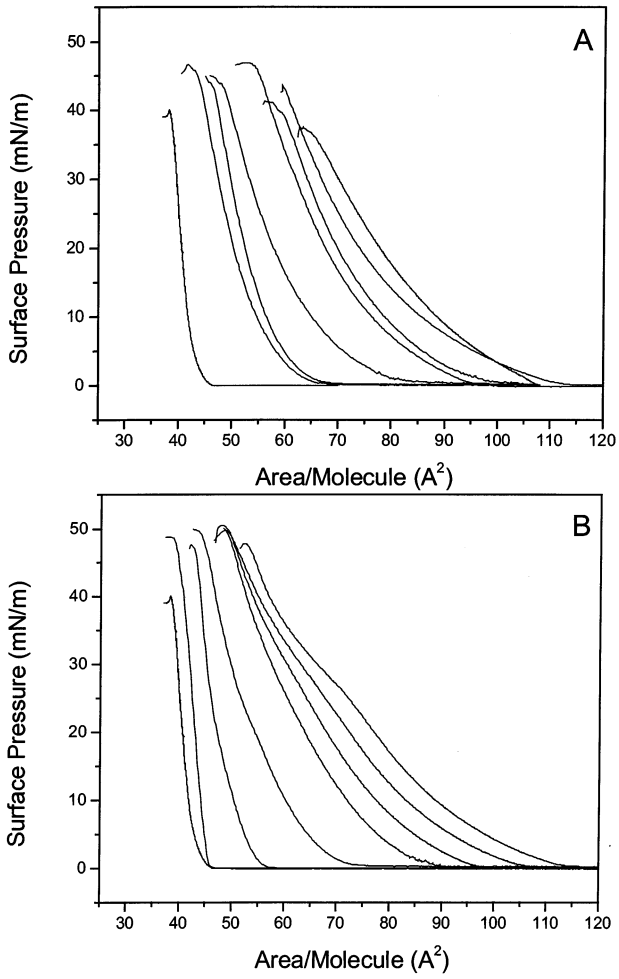

FIGURE 1: $\pi-A$ isotherms of (A) POPE−CHOL and (B) SM−CHOL mixed monolayers. χ_{CHOL} in POPE or SM (from right to left): 0, 0.05, 0.10, 0.20, 0.30, 0.40, 0.50, 1.0.

Table 1: A_{ideal} and A_{obs}, A_{lipid}, and Percent Condensation Values for Varying Mole Fractions χ_{CHOL} in POPE or SM $\pi-A$ Isotherms at 35 mN/m Surface Pressure[a]

lipid	χ_{CHOL}	A_{ideal} (Å^2)	A_{obs} (Å^2)	A_{lipid} (Å^2)	% condensation
POPE	0	−	65.2	65.2	−
	0.05	63.9	64.0	62.1	0.0
	0.10	62.6	61.4	57.5	1.8
	0.20	60.0	58.5	50.7	2.4
	0.30	57.3	51.4	39.8	10.3
	0.40	54.6	48.1	32.6	12.1
	0.50	52.0	45.4	26.0	12.6
SM	0	−	61.1	61.1	−
	0.05	60.0	58.8	56.9	1.9
	0.10	58.8	57.3	53.4	2.6
	0.20	56.6	55.1	47.3	2.6
	0.30	54.4	48.1	36.5	11.6
	0.40	52.2	44.0	28.5	15.6
	0.50	49.9	40.1	20.7	18.7

[a] Calculation of A_{ideal} and percent condensation is described under Experimental Procedures.

(*34*). Both $\pi-A$ isotherm measurements on monolayers and DSC measurements on bilayers indicate strong affinity between cholesterol and SM or POPE.

In the past, studies have indicated that cholesterol has a destabilizing effect upon PE lipids in model membranes (*35*). In addition, CHOL has been reported to have far less affinity for PEs in comparison to SM and PCs (*16*, *36*). Huang et al.

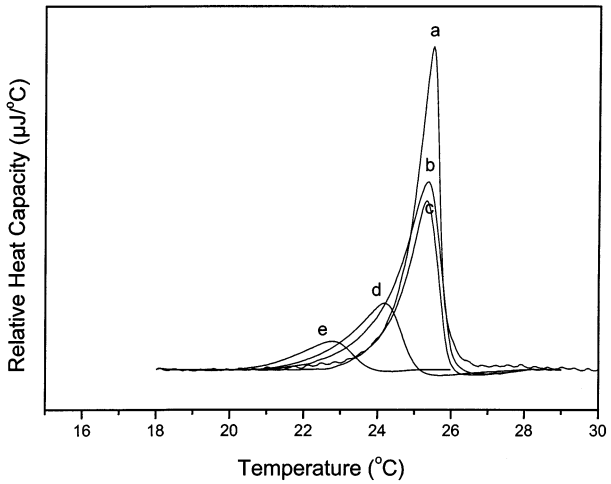

FIGURE 2: Effect of CHOL on DSC heating scans of MLVs made from POPE. χ_{CHOL} = (a) 0, (b) 0.0050, (c) 0.01, (d) 0.05, and (e) 0.10.

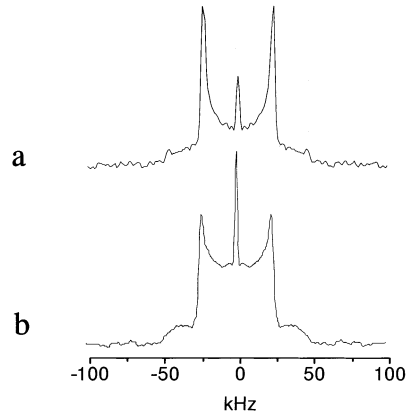

FIGURE 3: ^{2}H NMR spectra of 50 wt % aqueous multilamellar dispersions in 50 mM Tris (pH 7.4) at 35 °C for (A) POPE/[3α-$^2H_1$]CHOL (1:1 mol) and (B) SM/[3α-$^2H_1$]CHOL (1:1 mol).

reported cholesterol's solubility in POPE bilayers to be χ_{CHOL} = 0.51 whereas PC bilayers had a χ_{CHOL} = 0.66 solubility limit (*23*). Our $\pi-A$ isotherm data are consistent with the finding that CHOL is somewhat less miscible in POPE than SM. However, it does not appear to have a destabilizing effect on POPE monolayers. Pare and Lafleur also found that at high levels of CHOL ($\chi_{CHOL} \geq 0.35$) in POPE a l_o phase can be formed (*37*). They showed that the molecular organization of POPE-d_{31} bilayers containing $\chi_{CHOL} \geq 0.35$ was similar to that of PCs (*37*).

Molecular Organization of Cholesterol in POPE vs SM. Figure 3 presents ^{2}H NMR powder patterns at 35 °C of POPE/[3α-$^2H_1$]CHOL (1:1 mol) and SM/[3α-$^2H_1$]CHOL (1:1 mol) collected in order to compare any differences in the molecular organization of CHOL in the two bilayers. The powder patterns are typical of labeled CHOL in membranes. They consist of a powder pattern with a superimposed narrow central peak due to residual ^{2}HHO. The quadrupolar splittings $\Delta\nu_r$ = 46 ± 1 kHz calculated for [3α-$^2H_1$]CHOL in POPE (Figure 3A) and SM (Figure 3B) were identical within experimental uncertainty, corresponding to a tilt angle α_o = 16° ± 1° for the steroid moiety. A similar orientation has been previously reported in *sn*-1 saturated *sn*-2 unsaturated phospholipids (*38*). At equimolar concentrations, the organization of CHOL appears to be identical in both POPE and SM bilayers.

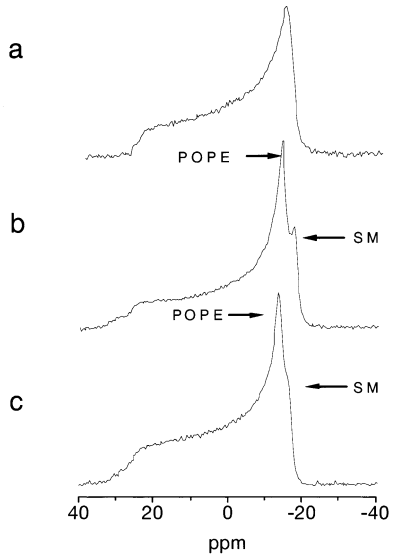

FIGURE 4: ^{1}H-decoupled ^{31}P NMR spectra for 50 wt % aqueous multilamellar dispersions in 50 mM Tris (pH 7.4) at 35 °C of (a) POPE, (b) POPE/SM (1:1 mol), and (c) POPE/SM/CHOL (1:1:1 mol). Chemical shifts are relative to external H_3PO_4 (85%).

Table 2: Chemical Shift Anisotropy ($\Delta\sigma_{csa}$) Values for Varying Lipid Compositions in Multilamellar Dispersions at 35 °C

lipid composition	$\Delta\sigma_{csa}$ (ppm)
POPE	40.5
SM	45.8
POPE/SM (1:1 mol)	40.5/50.3
POPE/SM/CHOL (1:1:1 mol)	39.8/47.3

Cholesterol's Effect on Headgroup Structures of POPE and SM Are Similar. We used ^{31}P NMR spectroscopy to examine the effect of CHOL on lipid packing in the headgroup region of POPE. Figure 4 shows the ^{1}H-decoupled ^{31}P NMR spectra for POPE, POPE/SM (1:1 mol), and POPE/SM/CHOL (1:1:1 mol) bilayers at 35 °C. They are powder patterns typical of phospholipid membranes in the L_α phase (*39*). Their shape is characterized by a low-frequency shoulder and a well-defined edge at high frequency, respectively, corresponding to parallel and perpendicular orientations of the bilayer normal relative to the magnetic field. The chemical shift anisotropy (Table 2) derived from the data by simulation for POPE (Figure 4a) is $\Delta\sigma_{csa}$ = 40.5 ppm, while the value is $\Delta\sigma_{csa}$ = 45.8 ppm for SM (spectrum not shown). These values are comparable with those previously measured for phospholipids in the L_α state (*35*, *40*).

The ^{31}P NMR spectrum for POPE/SM (1:1 mol) observed in the absence of CHOL (Figure 4b) consists of an inner powder pattern due to POPE superimposed upon a somewhat broader, outer powder pattern due to SM. Because POPE and SM share the same isotropic chemical shift (σ_{iso} = 0 ± 1 ppm) (*41*), a superposition of chemical-shifted powder patterns was ruled out. Our assignment conforms to the smaller chemical shift anisotropy measured for pure POPE (Figure 4a) bilayers, and was verified by ^{31}P NMR spectra that were collected on varying mixtures of POPE/SM (data not shown). The chemical shift anisotropy calculated for each component was, respectively, $\Delta\sigma_{csa}$ = 40.5 ppm and $\Delta\sigma_{csa}$ = 50.3 ppm (Table 2). We interpret the spectrum for the mixed sample (Figure 4b) in terms of a uniform distribution of POPE and SM molecules within the bilayer of a single lamellar phase. Perturbation to the conformation of the SM

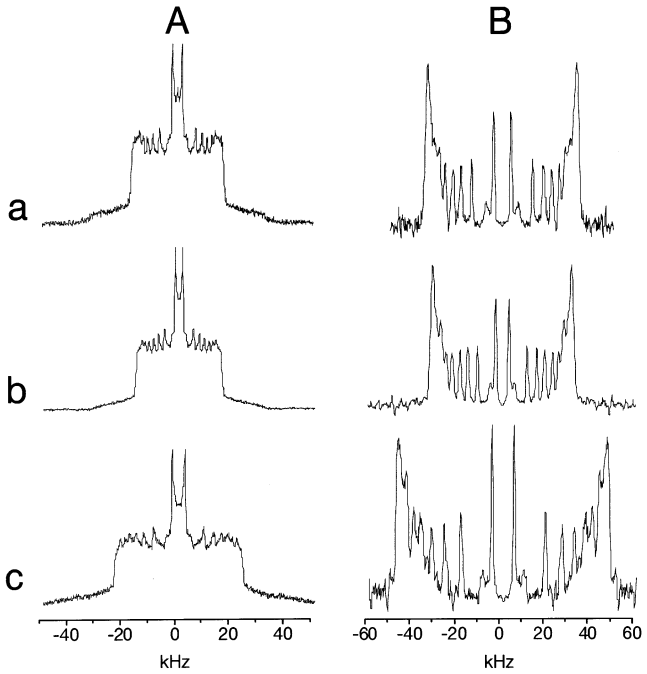

FIGURE 5: (A) ^{2}H NMR spectra of 50 wt % aqueous multilamellar dispersions in 50 mM Tris (pH 7.4) at 35 °C for (a) POPE-d_{31}, (b) POPE-d_{31}/SM (1:1 mol), and (c) POPE-d_{31}/SM/CHOL (1:1:1 mol). (B) Corresponding FFT depaked spectra of (a) POPE-d_{31}, (b) POPE-d_{31}/SM (1:1 mol), and (c) POPE-d_{31}/SM/CHOL (1:1:1 mol).

headgroup, which is indicative of intimate mixing with POPE, is implied by a change in chemical shift anisotropy relative to membranes prepared from the individual lipids. The absence of a change in chemical shift anisotropy for POPE in the mixed system is somewhat surprising. A possibility is that the conformational insensitivity to the presence of SM suggested for the PE headgroup arises from its smaller size. Similar two-component ^{31}P NMR spectra have been discerned with PC−PE mixtures (*40*, *42*−*44*). The consensus is that both species of these phospholipids adopt a common liquid-crystalline phase, although a possibility of nonrandom organization has been suggested (*42*). ^{31}P NMR spectra from soya PE−bovine brain SM membranes in the lamellar phase, in contrast, exhibited only a single component (*17*). Close similarity in chemical shift anisotropy was presumably responsible in this case.

The spectrum plotted for POPE/SM/CHOL (1:1:1 mol) bilayers in Figure 4c identifies that cholesterol affects the spectral component ascribed to POPE as well as SM. Visual inspection clearly reveals that resolution of the two powder patterns is diminished. Analysis yields $\Delta\sigma_{csa} = 39.8$ ppm for POPE and $\Delta\sigma_{csa} = 47.3$ ppm for SM (Table 2), establishing a reduction in chemical shift anisotropy of ∼1 ppm vs ∼3 ppm for the respective lipids due to introduction of the sterol. The implication is that cholesterol molecules have a very slight preference to insert into the mixed bilayer next to SM than POPE in the headgroup region. This statement, however, presumes linearity in the response to cholesterol concentration and equivalence in the incremental effect on the chemical shift anisotropy for each phospholipid. Neither presumption may be valid. An alternative explanation could be that the chemical shift anisotropy of PE is less sensitive to perturbation by cholesterol than SM.

Cholesterol Affects the Hydrocarbon Structure of POPE Even in the Presence of SM. Figure 5 A shows ^{2}H NMR spectra for POPE-d_{31}, POPE-d_{31}/SM (1:1 mol), and POPE-d_{31}/SM/CHOL (1:1:1 mol) at 35 °C. The spectra for all three lipid combinations are characteristic of the L_α phase. The spectrum for POPE-d_{31} (Figure 5a, panel A) exhibits sharp well-defined edges at about ±15 kHz corresponding to a region of essentially constant order in the upper part of the palmitoyl chain. The peaks are due to individual segments in the lower part of the acyl chain where the order gradually decreases toward the terminal methyl responsible for the central pair. Addition of equimolar SM to POPE-d_{31} qualitatively shows a similar spectrum with edges at ±15 kHz (Figure 5b, panel A). In the presence of CHOL [POPE-d_{31}/SM/CHOL (1:1:1 mol)] (Figure 5c, panel A), the edges of the spectrum are broadened to approximately ±23 kHz. This broadening indicates addition of CHOL increases the order of the palmitoyl chain of POPE in the mixed membrane.

Depaked ^{2}H NMR spectra are also presented in Figure 5 (panel B), where the enhanced resolution achieved is clearly apparent. They consist of 5−6 well-resolved doublets and an outermost composite doublet. The 5−6 doublets correspond sequentially with increasing splitting $\Delta\nu(\vartheta)$ to the terminal methyl and adjacent methylenes in the lower portion of the acyl chain (*24*). The composite doublet can be assigned to the ordered methylenes found in the upper part of the acyl chain.

Table 3: Data Derived from ^{2}H NMR Spectra Obtained for Multilamellar Dispersions at 35 °C[a]

lipid composition	M_1 ($\times 10^4$ s^{-1})	$\bar{S}_{CD}$	$\langle L\rangle$ (Å)	area (Å^2)
POPE-d_{31}	7.34	0.241	14.2	64.0
POPE-d_{31}/SM (1:1 mol)	6.36	0.209	13.5	66.8
POPE-d_{31}/SM/CHOL (1:1:1 mol)	9.97	0.327	15.8	57.3
PDPE-d_{31}	1.87	0.123	11.9	79.7
PDPE-d_{31}/CHOL (1:1 mol)	2.41	0.158	12.6	75.4
PDPE-d_{31}/SM (1:1 mol)	5.02	0.165	12.7	74.7
PDPE-d_{31}/SM/CHOL (1:1:1 mol)	6.35	0.208	13.5	70.1

[a] Calculation of average length $\langle L\rangle$ and average area $\langle A\rangle$ is described under Experimental Procedures. It should be noted that a factor of 1/2 was introduced into the right-hand side of eq 8 relating M_1 to $\bar{S}_{CD}$ for PDPE-d_{31} and PDPE-d_{31}/CHOL (1:1 mol) in the H_{II} phase (*49*). Experimental uncertainty in the values is 1−2%.

The first moment M_1 and average order parameter $\bar{S}_{CD}$ calculated by means of eqs 7 and 8, respectively, from the ^{2}H NMR spectra are presented in Table 3. The average acyl chain length $\langle L\rangle$ (eq 9) was derived from $\bar{S}_{CD}$ for all lipid combinations examined (Table 3) at 35 °C. The values of $\langle L\rangle$ calculated for POPE-d_{31}, POPE-d_{31}/SM (1:1 mol), and POPE-d_{31}/SM/CHOL (1:1:1 mol) were 14.2, 13.5, and 15.8 Å, respectively. The sharp increase in $\langle L\rangle$ observed with the addition of CHOL is consistent with previous findings that CHOL increases bilayer thickness (*14*). This increase in thickness is thought to be a result of CHOL restricting trans-gauche isomerizations within the acyl chains. The areas/molecule calculated for POPE-d_{31} (eq 10) from the ^{2}H NMR data are presented in Table 3. The value is $A = 64.0$ Å^2 in single-component POPE-d_{31}. In POPE-d_{31}/SM (1:1 mol), $A = 66.8$ and 57.3 Å^2, respectively, without and with the addition of equimolar CHOL.

Our $\bar{S}_{CD}$ values for POPE-d_{31} and POPE-d_{31}/SM (1:1 mol) are similar to those reported by Pare and Lafleur (*37*). They found $\bar{S}_{CD} \sim 0.22$ in POPE-d_{31} at 32 °C, while we measure $\bar{S}_{CD} = 0.241$ for POPE-d_{31} and $\bar{S}_{CD} = 0.209$ for POPE/SM

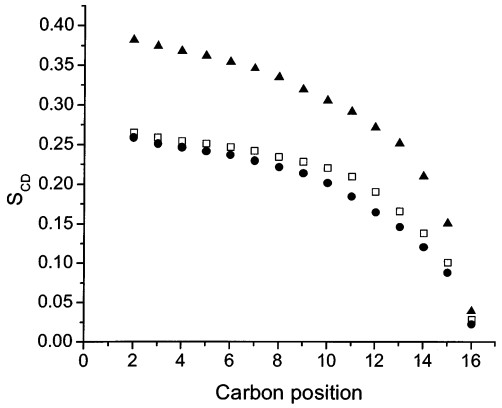

FIGURE 6: Smoothed order parameter profiles for POPE-d_{31} (□), POPE-d_{31}/SM (1:1) (●), and POPE-d_{31}/SM/CHOL (1:1:1) (▲) at 35 °C. Order parameters were calculated using eq 11 and assigned on the basis of integrated intensity assuming monotonic variation.

(1:1 mol) at 35 °C. A comparison of the effect of cholesterol seen in the two studies is informative. The $\bar{S}_{CD}$ value of 0.327 measured here for POPE-d_{31}/SM/CHOL (1:1:1 mol) at 35 °C corresponds to an increase of >50% relative to the CHOL-free system, which compares with an increase of ~37% reported upon incorporation of 45 mol % CHOL into POPE-d_{31} (POPE-d_{31}/CHOL 1:0.8) at 32 °C. Strong interaction between sterol and PE is implied irrespective of the presence of SM.

The depaked data were utilized to calculate bond order parameters ($\bar{S}_{CD}$) at 35 °C as a function of acyl chain position in POPE-d_{31}, POPE-d_{31}/SM (1:1 mol), and POPE-d_{31}/SM/CHOL (1:1:1 mol) (Figure 6). The order parameter profiles were generated by assigning equal integrated intensity to each methylene group of the palmitoyl chain and assuming that order decreases monotonically toward the terminal methyl (*31*). They display a characteristic plateau region of nearly constant order in the upper part of the palmitoyl chain followed in the lower portion by a progressive decrease in order toward the center of the bilayer. Although all three profiles show the same qualitative trend, differences in magnitude exist between the profiles. The addition of equimolar SM to POPE-d_{31} results in a slight lowering of $\bar{S}_{CD}$ throughout the chain, which is consistent with the small reduction measured in $\bar{S}_{CD}$ (Table 3). The profile demonstrates that the lowering is most marked in the middle section of the acyl chain. In contrast, including equimolar cholesterol in POPE-d_{31}/SM (1:1 mol) greatly increases the order at all carbon positions. The plateau region is raised from $\bar{S}_{CD} \sim 0.25$ to $\bar{S}_{CD} \sim 0.37$, while toward the center of the membrane the differential becomes less. These changes in $\bar{S}_{CD}$ values are comparable to those found for the affect of CHOL on POPE-d_{31} in the absence of SM (*37*). Pare and Lafleur reported that the addition of $\chi_{CHOL} = 0.45$ (POPE-d_{31}/CHOL 1:0.8) increased $\bar{S}_{CD}$ in the plateau region from ~0.26 to ~0.36. The findings are consistent with the known effect of CHOL on phospholipid membranes. The rigid nonpolar planar molecule restricts lipid chain motion by diminishing trans-gauche isomerization (*10*).

A recent publication on the effect of cholesterol on a POPC/SM (1:3 mol) mixture that mimics the lipid composition of the external leaflet of renal brush-border membranes concluded that at high content the sterol acts as a suppressor rather than as a promoter of domains (*45*). DSC and AFM

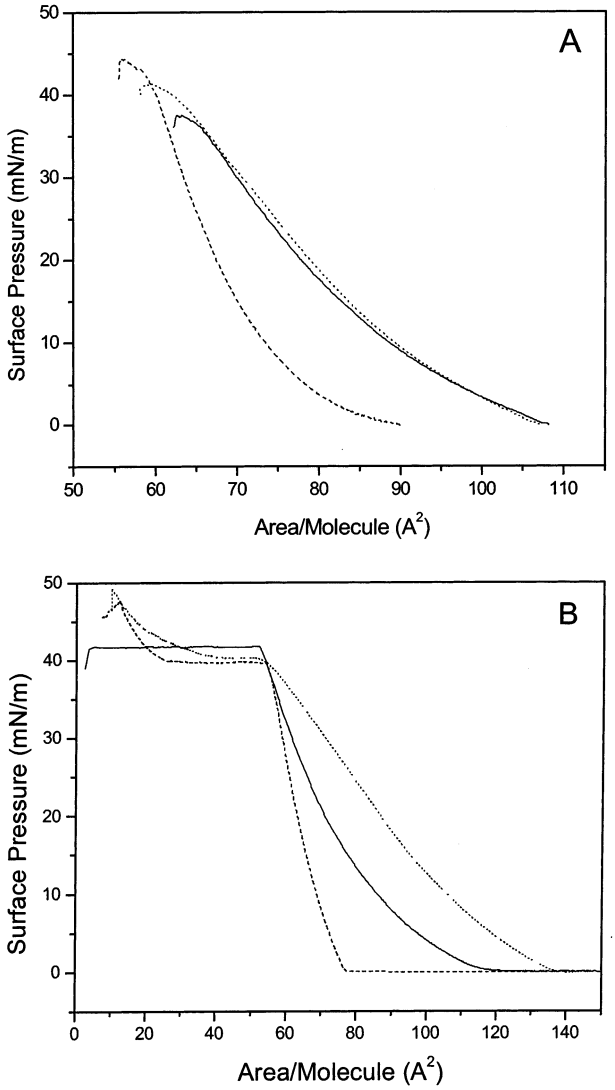

FIGURE 7: $\pi-A$ isotherms obtained at 35 °C of (A) POPE (solid line), POPE/SM (1:1 mol) (dotted line), and POPE/SM/CHOL (1:1:1 mol) (dashed line), and (B) PDPE (solid line), PDPE/SM (1:1 mol) (dotted line), and PDPE/SM (1:1 mol) with $\chi_{CHOL} = 0.20$ (dashed line) mixed monolayers.

evidence in favor of phase separation into domains was presented up to 33 mol % cholesterol. No domains were seen beyond this concentration. We cannot rule out analogous behavior in our POPE/SM (1:1 mol) system. The cholesterol-associated perturbation of the *sn*-1 chain of POPE seen in POPE-d_{31}/SM/CHOL (1:1:1 mol) could result if a similar threshold applies at lower sterol content. It is also possible that SM-rich domains exist, but are saturated with cholesterol. The perturbation to PE could then be due to sterol excluded from these domains. However, the similarity in response to cholesterol manifest by POPE and SM does not offer a strong molecular rationale for such scenarios.

Role for Polyunsaturated Lipids in Phase Separation. Our results on POPE−SM neither detect phase separation of the two lipids nor imply preferential interaction of cholesterol with SM. In contrast, we have previously reported that SM and SM−CHOL clusters phase-separate from phospholipids containing polyunsaturated acyl chains (*34*). Here we first compare differences in monolayer behavior between POPE and the DHA-containing phospholipid PDPE. Figure 7 (panel A) shows $\pi-A$ isotherms for POPE, POPE/SM (1:1 mol),

and POPE/SM/CHOL (1:1:1 mol). At 35 mN/m of surface pressure, the area/molecule values respectively for POPE, POPE/SM (1:1 mol), and POPE/SM/CHOL (1:1:1 mol) were 65.2, 66.6, and 61.4 Å^2. These values from $\pi-A$ isotherms qualitatively follow the same trend exhibited by the average area/molecule values calculated from the ^{2}H NMR data for POPE-d_{31} in bilayers of equivalent composition (Table 3).

Figure 7 (panel B) shows $\pi-A$ isotherms for PDPE, PDPE/SM (1:1 mol), and PDPE/SM (1:1 mol) with $\chi_{CHOL} = 0.20$. At $\chi_{CHOL} > 0.20$, there was monolayer collapse, indicating monolayer instability, and the isotherms are not shown. A clear distinction between PDPE vs POPE is apparent. The $\pi-A$ isotherms in the presence of PDPE all contain a plateau (near-horizontal) region at a surface pressure of ~40 mN/m, indicating squeeze out or molecular loss. Although it is possible that part of a plateau may be attributed to chain ordering transitions, we verified the squeeze out hypothesis by obtaining $\pi-A$ isotherms in the presence of PDPE at varying temperatures (data not shown). The lateral surface pressure for each plateau remained the same at all temperatures examined, indicating squeeze out as opposed to a first-order chain transition. We (*34*, *46*) and others (*21*, *47*) have previously described the concept of squeeze out from Langmuir−Blodgett films. For pure PDPE, the plateau region at 41 mN/m of surface pressure continues from an area/molecule = 52.1 Å^2 until the barriers touch. The $\pi-A$ isotherm following addition of equimolar SM to PDPE exhibits a near-horizontal plateau region from an area/molecule = 52.0 to 38.6 Å^2, suggesting phase separation between PDPE and SM (Figure 7). Introducing $\chi_{CHOL} = 0.20$ into PDPE/SM (1:1 mol) increased the plateau region from an area/molecule = 54.2 to 24.7 Å^2, suggesting enhanced phase separation due to the presence of the sterol. We quantified the number of molecules lost or squeezed out (eq 4) for PDPE/SM (1:1 mol) and PDPE/SM/CHOL (1:1:0.2 mol) to be 25.9% and 54.4%, respectively, in the plateau region. It can be seen for the mixed $\pi-A$ isotherms that after the PDPE is squeezed out, the pressure continues to rise, showing monolayers that are primarily SM or SM−CHOL. Therefore, the near-horizontal regions in the $\pi-A$ isotherms are not monolayer collapse but a preferential squeeze out of PDPE or PDPE−SM.

We investigated phase separation between PDPE and SM in bilayers using DSC in comparison to POPE−SM. Figure 8 (top) presents DSC heating scans for POPE/SM (1:1 mol) and POPE/SM/CHOL (1:1:0.0050 mol). The DSC scan of POPE/SM (1:1 mol) showed a broad single peak with a T_m = 25.1 °C, indicating no phase separation. Addition of χ_{CHOL} = 0.0050 to POPE/SM (1:1 mol) lowers the transition temperature slightly (T_m = 24.1 °C) and significantly decreases the enthalpy. DSC scans for PDPE, PDPE/SM (1:1 mol), and PDPE/SM/CHOL (1:1:0.0050 mol) are also presented in Figure 8 (bottom). The gel to liquid-crystalline phase transition in PDPE alone is sharp with a $T_m = 2.2$ °C. In contrast to POPE/SM (1:1 mol), an equimolar mixture of PDPE and SM results in a low-melting, PDPE-rich peak and a high-melting SM-rich peak with T_m values of 11.9 and 24.2 °C, respectively. Phase separation between PDPE and SM is the implication. Addition of $\chi_{CHOL} = 0.0050$ obliterates the enthalpy of the high-melting SM-dependent peak while the enthalpy of the low-melting PDPE-dependent peak remains unchanged. Further addition of cholesterol (χ_{CHOL} > 0.01) eventually obliterates the PDPE-rich peak as well (*34*). The DSC data suggest a larger affinity of cholesterol for SM than for PDPE at low levels of sterol that is not evident at high cholesterol concentrations, where most studies have been performed (*11*, *48*). Clearly, the organization of cholesterol at low levels needs to be investigated extensively and may be fruitful toward understanding domain formation.

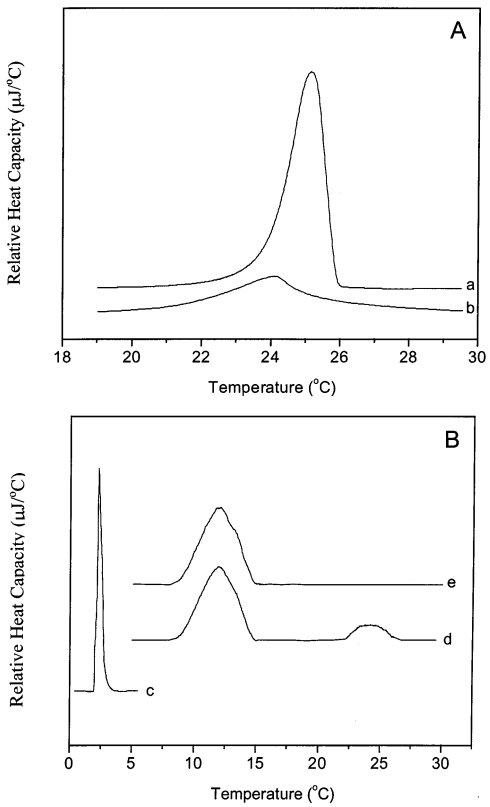

FIGURE 8: DSC heating scans of MLVs made from (A) (a) POPE/SM (1:1 mol) and (b) POPE/SM (1:1 mol) with $\chi_{CHOL} = 0.005$; (B) (c) PDPE, (d) PDPE/SM (1:1 mol), and (e) PDPE/SM (1:1 mol) with $\chi_{CHOL} = 0.005$.

To investigate the specific effect of cholesterol on the acyl chain organization of PDPE, ^{2}H NMR spectra were acquired for *sn*-1 chain perdeuterated PDPE-d_{31}. Figure 9 shows spectra of PDPE-d_{31}, PDPE-d_{31}/CHOL (1:1 mol), PDPE-d_{31}/SM (1:1 mol), and PDPE-d_{31}/SM/CHOL (1:1:1 mol) at 35 °C. Table 3 lists the values derived for M_1, $\bar{S}_{CD}$, and $\langle L \rangle$. The spectra for PDPE-d_{31} (Figure 9a) and PDPE-d_{31}/CHOL (1:1 mol) (Figure 9b) are characteristic of the inverted hexagonal (H_{II}) phase (*49*) with edges, respectively, at ±7 and ±9 kHz. They are reduced in width by a factor of 1/2 relative to powder patterns for the L_α phase because translational diffusion of lipid around the cylindrical structures that comprise the H_{II} phase provides additional motional averaging. A propensity to form this phase at physiological temperature has previously been reported for highly polyunsaturated SDPE (*25*). The approximate doubling in width of the spectra for PDPE-d_{31}/SM (1:1 mol) (Figure 9c) and PDPE-d_{31}/SM/CHOL (1:1:1 mol) (Figure 9d) demonstrates that the introduction of SM has induced PDPE to adopt the L_α phase. The respective edges of the spectra are ±17 and ±22 kHz.

Inspection of Table 3 reveals that addition of CHOL to PDPE-d_{31} in a 1:1 molar ratio and to PDPE-d_{31}/SM in a 1:1:1 molar ratio resulted in an increase in the average order

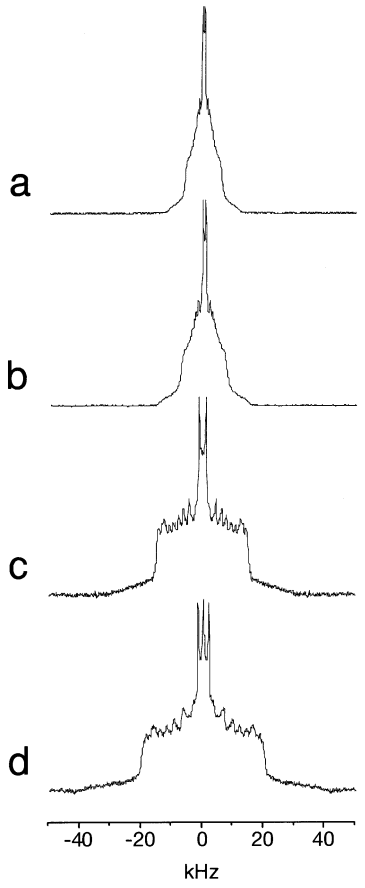

FIGURE 9: ^{2}H NMR spectra of 50 wt % aqueous multilamellar dispersions in 50 mM Tris (pH 7.4) at 35 °C for (a) PDPE-d_{31}, (b) PDPE-d_{31}/CHOL (1:1 mol), (c) PDPE-d_{31}/SM (1:1 mol), and (d) PDPE-d_{31}/SM/CHOL (1:1:1 mol).

parameter $\bar{S}_{CD}$. The increase in the latter system, in particular, was 26%. This figure compares with an increase of 57% seen when the same amount of CHOL was added to POPE-d_{31}/SM (1:1 mol). Although the sterol is ordering the palmitoyl *sn*-1 chain of PDPE-d_{31} in the presence of SM, the change is less than half that in POPE-d_{31}/SM. Segregation of cholesterol into SM-rich patches that are phase-separated from PDPE-rich regions is an interpretation consistent with our Langmuir trough and DSC data. Poor affinity of cholesterol for polyunsaturated acyl chains has been proposed previously to trigger domain formation within membranes (*22*, *50*−*52*). Huster et al. employed ^{2}H NMR to measure the increase in order of each phospholipid due to incorporation of 10 mol % cholesterol into SDPC/SDPE/SDPS (4:4:1 mol) and SOPC/SOPE/SOPS (4:4:1) mixtures (*51*). They detected a marked differential in ordering for SDPC-d_{31} in SDPC/SDPE/SDPS (4:4:1 mol) that was interpreted in terms of clustering into SDPC/sterol microdomains 250 Å in radius. In the same study, closer contact with the saturated *sn*-1 chain than with the polyunsaturated *sn*-2 chain was revealed for cholesterol by a higher rate of chain-to-sterol nuclear Overhauser enhancement spectroscopy (NOESY) cross-relaxation in ^{1}H magic angle spinning (MAS) NMR experiments on SDPC/cholesterol-*25*,*26*,*26*,*26*,*27*,*27*-d_7 (1:1 mol) bilayers. Pressure−area isotherms for 18:0,18:1PC/18:0, 22:6PC/cholesterol monolayers have also indicated that the sterol interacts less favorably with the polyunsaturated PC (*50*). Unequivocal evidence that cholesterol has poor affinity to polyunsaturated fatty acids comes from its low solubility in dipolyunsaturated phospholipid membranes where intimate contact is unavoidable (*22*, *38*, *51*). We attribute the sterol's tendency to avoid intimate contact with polyunsaturated fatty acids to steric incompatability between the rigid steroid moiety and the highly disorganized chain (*22*). A saturated or monounsaturated chain, on the other hand, would constitute a relatively smooth façade compatible with near-approach.

The possibility exists that a difference in acyl chain length between docosahexaenoic and oleic acids is responsible for the distinction in response to cholesterol identified here between PDPE/SM and POPE/SM, but is considered unlikely. Despite the four extra carbons in DHA, computer modeling of diacylglycerols containing stearic acid at the *sn*-1 position indicates a discrepancy of $<$1.5 Å in length for docosahexaenoic vs oleic scid at the *sn*-2 position (*53*). Our calculations of effective acyl chain length $\langle L \rangle$ in PDPE-d_{31}/SM (1:1 mol) and POPE-d_{31}/SM (1:1 mol) bilayers, moreover, are within $<$1 Å (Table 3).

Implications for Lipid Microdomains/Lipid Rafts. Recent studies have shown that in the presence of cholesterol, unsaturated phospholipids segregate from saturated phospholipids/sphingolipids due to relative affinities between acyl chains (*11*, *48*). Headgroup interactions appear to only play a modest role in lateral phase separations (*54*). Our findings with POPE−SM−CHOL and PDPE−SM−CHOL systems support the concept that lipid raft stability is conferred by acyl chain interactions. We saw no evidence with POPE to indicate that a monounsaturated PE phase-separates from SM and CHOL, which contradicts the behavior that would be expected on the basis of headgroup affinities. Wang and Silvius have previously reported that monunsaturated lipids do partition into l_o phases albeit less than saturated species (*54*). Upon introduction of polyunsaturation when POPE is substituted by PDPE, our preliminary observations from π−*A* isotherm and DSC studies indicate that phase separation of PDPE and SM results and that cholesterol possesses preferential affinity for SM. The ^{2}H NMR data for the PDPE-d_{31} mixtures imply that cholesterol's affinity for PDPE in the presence of SM is substantially smaller than for POPE. Our data suggest that lipid rafts of pure SM−CHOL entities may be an oversimplification. Rather, lipid rafts, in addition to SM and CHOL, must contain other lipid "contaminants", and all of these lipids probably exchange rapidly between domains.

Although SM−CHOL-rich lipid rafts and associated proteins that are found in DRMs have received much attention, relatively little is understood about the role of DHA-rich microdomains. The data presented here confirm the hypothesis that DHA-containing phospholipids may be involved in affecting different types of lipid microdomains (*22*, *55*, *56*). In addition, we propose that polyunsaturation may be involved in conferring raft stability. Our model has phase separation into DHA-rich CHOL-poor microdomains within DSMs promoting the formation of SM−CHOL-rich rafts. These microdomains may influence protein function, similar to the effect of lipid rafts on GPI-anchored proteins and SRC family of kinases. DHA has already been implicated in playing a role in protein functionality for rhodopsin (*56*) and nicotinic acetylcholine receptor (*57*), activation of phospholipase C and protein kinase C, and deactivation of protein kinase A (*58*). The impact of DHA on membrane

structure and protein functionality may therefore provide some understanding of DHA's global affect on numerous disease states (*55*). Primarily through epidemiological and dietary studies DHA has been positively linked to the alleviation of a variety of human afflictions including cancer, heart disease, rheumatoid arthritis, alcoholism, and depression (*55*). Clearly an understanding of the role of DHA in membrane structure may provide much insight into various cellular processes.

Conclusion. Our data establish that in equimolar mixtures of POPE−SM−CHOL, sterol and PE are in close proximity. There does not appear to be lateral phase separation into SM−CHOL-rich rafts. We attribute this behavior to a high degree of miscibility between POPE and CHOL which is retained in the presence of SM. However, our preliminary experiments demonstrate that replacing POPE with PDPE may result in SM phase separation from PDPE. This phase separation remains upon the addition of low cholesterol that preferentially interacts with SM as evidenced by our DSC data. Although our ^{2}H NMR experiments indicate that the cholesterol orders PDPE-d_{31} in PDPE/SM, the affinity to sterol implied is far less than for POPE-d_{31} in POPE/SM and may be critical to enhance phase separation. A crucial role for polyunsaturated DHA is implied, which supports the model that lipid raft stability is conferred by acyl chain structure. The role of DHA may be to enhance phase separation of l_o SM−CHOL-rich lipid rafts from the surrounding l_d phase. A better understanding of DHA-containing phospholipids is essential to explain the effects of DHA-rich CHOL-poor domains that may be involved in controlling the functionality of certain proteins. Current studies are underway to assess how DHA affects different membrane proteins.

ACKNOWLEDGMENT

We thank Dr. Stephanie Sen for her assistance in the synthesis of [3α-$^2H_1$]CHOL.

REFERENCES

1. Koval, M., and Pagano, R. E. (1991) *Biochim. Biophys. Acta 1082*, 113−125.
2. Straume, M. (1987) *Biochemistry 26*, 5121−5126.
3. Glaser, M. (1993) *Curr. Opin. Struct 3*, 475−481.
4. Welti, R., and Glaser, M. (1994) *Chem. Phys. Lipids 73*, 121−137.
5. Hooper, N. (1999) *Mol. Membr. Biol. 16*, 145−156.
6. Eddidin, M. (1993) *J. Cell Sci. 17*, 165−169.
7. Pralle, A., Keller, P., Florin, E. L., Simons, K., and Horber, J. K. H. (2000) *J. Cell Biol. 148*, 997−1008.
8. Brown, D. A., and London, E. (2000) *J. Biol. Chem. 275*, 17221−17224.
9. Simons, K., and Ikonen, E. (1997) *Nature* 569−572.
10. Brown, R. E. (1998) *J. Cell Sci. 111*, 1−9.
11. Ahmed, S. N., Brown, D. A., and London, E. (1997) *Biochemistry 36*, 10944−10953.
12. Brown, D. A., and Rose, J. K. (1992) *Cell 67*, 533−544.
13. Moffett, S., Brown, D. A., and Linder, M. E. (2000) *J. Biol. Chem. 275*, 2191−2198.
14. Samsonov, A. V., Mahalyov, I., and Cohen, F. S. (2001) *Biophys. J. 81*, 1486−1500.
15. McIntosh, T. J., Simon, S. A., Needham, D., and Huang. C. (1992) *Biochemistry 31*, 2012−2020.
16. Van Dijck, P. M. W., De Kruijff, B. B. K., Van Deenen, L. L. M., De Gier, J., and Demel, R. A. (1976) *Biochim. Biophys. Acta 455*, 576−587.
17. Cullis, P. R., and Hope, M. J. (1980) *Biochim. Biophys. Acta 597*, 533−542.
18. Oldfield, E., Meadows, M., Rice, D., and Jacobs, R. (1978) *Biochemistry 17*, 2727−2740.
19. Smaby, J. M., Brockman, H. L., and Brown, R. E. (1994) *Biophys. J. 73*, 1492−1505.
20. Smaby, J. M., Momsen, M., Kulkarni, V. S., and Brown, R. E. (1996) *Biochemistry 35*, 5696−5704.
21. Boonman, A., Machiels, F. H. J., Snik, A. F. M., and Egberts, J. (1987) *J. Colloid Interface Sci. 120*, 456−468.
22. Brzustowicz, M. R., Cherezov, V., Caffrey, M., Stillwell, W., and Wassall, S. R. (2002) *Biophys. J. 82*, 285−298.
23. Huang, J., Buboltz, J. T., and Feigenson, G. W. (1999) *Biochim. Biophys. Acta 1417*, 89−100.
24. McCabe, M. A., Griffith, G. L., Ehringer, W. D., Stillwell, W., and Wassall, S. R. (1994) *Biochemistry 33*, 7203−7210.
25. Shaikh, S. R., Brzustowicz, M. R., Stillwell, W., and Wassall, S. R. (2001) *Biochem. Biophys. Res. Commun. 286*, 758−763.
26. Davis, J. H. (1983) *Biochim. Biophys. Acta 737*, 117−171.
27. Holte, L. L., Peter, S. A., Sinnwell, T. M., and Gawrisch, K. (1995) *Biophys. J. 68*, 2396−2403.
28. Nagle, J. F. (1993) *Biophys. J. 64*, 1476−1481.
29. Marsh, D. (1992) *CRC Handbook of Lipid Bilayers*, CRC Press, Boca Raton, FL.
30. McCabe, M. A., and Wassall, S. R. (1997) *Solid State Nucl. Magn. Reson. 10*, 53−61.
31. Lafleur, M., Fine, B., Sternin, E., Cullis, P. R., and Bloom, M. (1989) *Eur. Biophys. J. 56*, 1037−1041.
32. Dietrich, R., and Trahms, L. (1987) *J. Magn. Reson. 71*, 337−341.
33. Phillips, M. C., and Chapman, D. (1968) *Biochim. Biophys. Acta 163*, 301−313.
34. Shaikh, S. R., Dumaual, A. C., Jenski, L. J., and Stillwell, W. (2001) *Biochim. Biophys. Acta 1512*, 317−322.
35. Cullis, P. R., Van Dijck, P. M. W., D., De Kruijff, B., and De Gier, J. (1978) *Biochim. Biophys. Acta 513*, 21−30.
36. Van Dijck, P. W. M. (1979) *Biochim. Biophys. Acta 555*, 89−101.
37. Pare, C., and Lafleur, M. (1998) *Biophys. J. 74*, 899−909.
38. Brzustowicz, M. R., Stillwell, W., and Wassall, S. R. (1999) *FEBS Lett. 451*, 197−202.
39. Seelig, J. (1978) *Biochim. Biophys. Acta 515*, 105−140.
40. Ghosh, R. (1988) *Biochemistry 27*, 7750−7758.
41. Yeagle, P. L. (1987) in *Phosphorus NMR in Biology* (Burt, C. T., Ed.) pp 95−133, CRC Press, Inc., Boca Raton, FL.
42. Arnold, K., Lösche, A., and Gawrisch, K. (1981) *Biochim. Biophys. Acta 645*, 143−148.
43. Eriksson, P.-O., Rilfors, L., Lindblom, G., and Arvidson, G. (1985) *Chem. Phys. Lipids 37*, 357−371.
44. Separovic, F., and Gawrisch, K. (1996) *Biophys. J. 71*, 274−282.
45. Milhiet, P. E., Giocondi, M. C., and Grimellec, C. L. (2002) *J. Biol. Chem. 22*, 875−878.
46. Dumaual, A. C., Jenski, L. J., and Stillwell, W. (1999) *Biochim. Biophys. Acta 1463*, 395−406.
47. Egberts, J., Sloot, H., and Mazure, A. (1989) *Biochim. Biophys. Acta 1002*, 109−113.
48. Dietrich, C., Bagatolli, L. A., Volovyk, Z. N., Thompson, N. L., Jacobson, K., and Gratton, E. (2001) *Biophys. J. 80*, 1417−1428.
49. Thurmond, R. L., Lindblom, G., and Brown, M. R. (1993) *Biochemistry 32*, 5394−5410.
50. Zerouga, M., Jenski, L. J., and Stillwell, W. (1995) *Biochim. Biophys. Acta* 1236, 266−272.
51. Huster, D., Arnold, K., and Gawrisch, K. (1998) *Biochemistry 37*, 17299−17308.
52. Mitchell, D. C., and Litman, B. J. (1998) *Biophys. J. 74*, 879−891.
53. Applegate, K. R., and Glomset, J. A. (1991) *J. Lipid Res. 32*, 1635−1644.
54. Wang, T., Leventis, R., and Silvius, J. R. (2000) *Biophys. J. 79*, 919−933.
55. Stillwell, W. (2000) *Curr. Org. Chem. 4*, 1169−1183.
56. Litman, B. J., and Mitchell, D. C. (1996) *Lipids 31*, 193−197.
57. Rankin, S. E., Addona, G. H., Kloczewiak, M. A., Bugge, B., and Miller, K. W. (1997) *Biophys. J. 73*, 2446−2455.
58. Padma, M., and Das, U. N. (1999) *Prostaglandins, Leukotrienes Essen. Fatty Acids 60*, 55−63.

BI025712B